EXTERNAL MAGNETIC FIELDS AS SEEN FROM THE SURFACE WITH INSIGHT. Anna Mittelholz[1], C. L. Johnson[2,3], S. N. Thorne[2], P. Chi[4], M. O. Fillingim[5], S. Joy[4], R. Lorenz[6], A. Spiga[7,8], S. E. Smrekar[9], W. B. Banerdt[9], [1]ETH Zurich, Switzerland (amittelholz@erdw.ethz.ch). [2]Planetary Science Institute, Tucson, AZ 85719, USA. [3]Dept. of Earth, Ocean and Atmospheric Sciences, University of British Columbia, Vancouver, BC, V6T 1Z4, Canada. [4]Earth, Planetary and Space Sciences, UCLA, Los Angeles, CA, USA. [5]Space Sciences Laboratory, University of California, Berkeley, CA, USA. [6]Johns Hopkins Applied Physics Laboratory, Laurel, MD, USA. [7]Laboratoire de Météorologie Dynamique / Institut Pierre Simon Laplace, Sorbonne Université, CNRS, École Polytechnique, ENS, Paris, France. [8]Institut Universitaire de France, Paris, France. [9]Jet Propulsion Laboratory, Pasadena, CA 91109, USA.

Introduction: InSight landed on Mars in November 2018 [1] and includes in its payload the InSight FluxGate Magnetometer, IFG. Although the IFG is part of the Auxiliary Payload Sensor Suite, meant to characterize the environment around the lander, the instrument has provided the first surface magnetic field measurements on Mars [2], [3]. As such, scientific achievements from the IFG have been an important mission contribution.

Magnetic fields measured by the IFG comprise external and internal fields, generated outside or inside the planetary body respectively. Strong crustal fields provide evidence for an ancient dynamo. The IFG measured a surface magnetic field strength of ~2000 nT, ten times stronger than predicted from satellite data [2], [4] and consistent with a dynamo of Earth-like strength [2]. Furthermore, we have observed time-varying external fields at the planetary surface that after estimation and subtraction of lander-generated fields include contributions with different periods and origins.

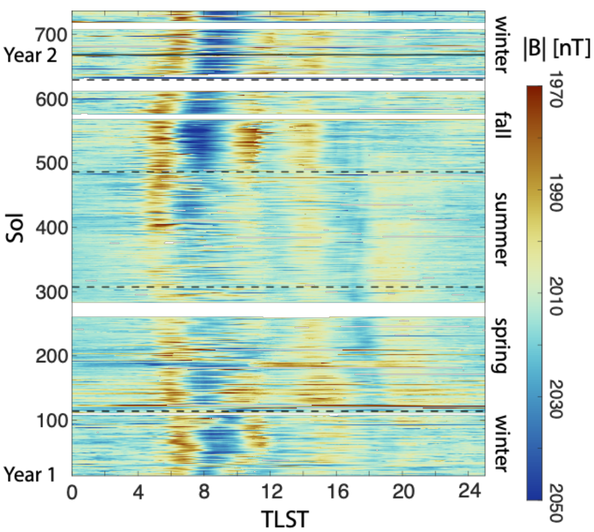

Figure 1 The magnetic field amplitude, |B|, versus true local time (TLST) from sol 14-736 of InSight operations. Data is binned in 30-s-time bins and the mean in each bin is shown. Dashed lines are solstices and equinoxes in the northern hemisphere. The solid line marks sol 668 and the beginning of year 2 on Mars.

External fields have been observed and characterized from orbit (e.g. [5]–[7]), specifically with the Mars Global Surveyor (MGS) and Mars Atmosphere and Volatile EvoutioN (MAVEN) missions. However, the degree to which external fields penetrate to and interact with the surface could not be studied prior to the InSight landing. Here, we present an overview of surface magnetic field observations that indicate different external magnetic field phenomena, transient and periodic, throughout the first 736 sols of InSight operations. Some of those phenomena have been reported previously [2], [9]–[14] but are included to provide a comprehensive overview.

Data: IFG data for sols 14-736 (Fig. 1) have been collected almost continuously. Some data gaps exist due to electronics anomalies [1,2] and power constraint related switch-offs. Continuous data exist at 0.2 Hz for the beginning of the mission, and the sampling rate was increased to 2 Hz at sol 179 [12]. Here, we use data in the Mars Solar Orbital (MSO) frame in which *X* points from Mars towards the Sun, *Y* points anti-parallel to Mars' orbital velocity vector and *Z* completes the right-handed system.

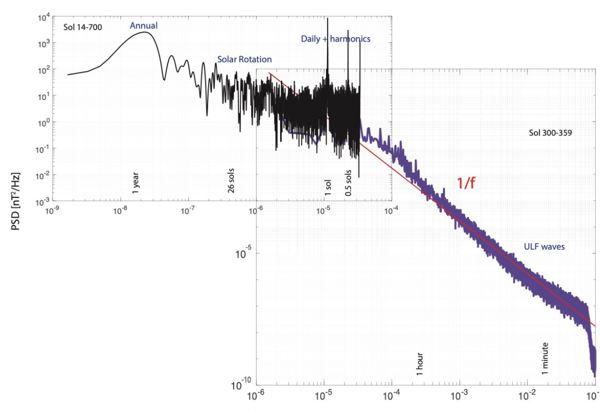

Figure 2 A composite power spectral density (PSD) plot for the surface magnetic field strength at the InSight landing site. PSD estimates for longer periods are derived using a Lomb-Scargle algorithm (black) for sols 14-700. The shorter periods (purple) show a Welch PSD spectrum for sols 300-359, a time period for which no large data gaps occurred.

Observation: We describe a range of physical phenomena leading to magnetic field signals with periodicities ranging from less than 1 minute to annual (Fig. 2), as well as transient signals.

Annual / Seasonal: The more than one martian year of InSight data enable detection of seasonal variations in the data, although robust characterization of these would require multiple years of data. We previously explored diurnal fields [13], [14], and found that seasonal variations in these result in increased peak amplitudes during the fall and winter. This effect was shown to be enhanced during seasonal dust storms.

Solar Rotation: Variations due to the solar rotation are expected to occur with a period of ~26 days. Because of data gaps of variable length, we exploit the Lomb-Scargle method for spectral analyses. For comparison, we also perform a spectral analysis of MAVEN data in the undisturbed solar wind (Fig. 3). Orbital data shows an IMF signature mostly in the horizontal component (reflecting draped IMF field lines around the planetary obstacle). IFG data unexpectedly show a peak at ~26 days in the B_X component which points towards the Sun. We hypothesize that this might be related to the interaction of IMF field lines with the crustal magnetic field at the InSight landing site.

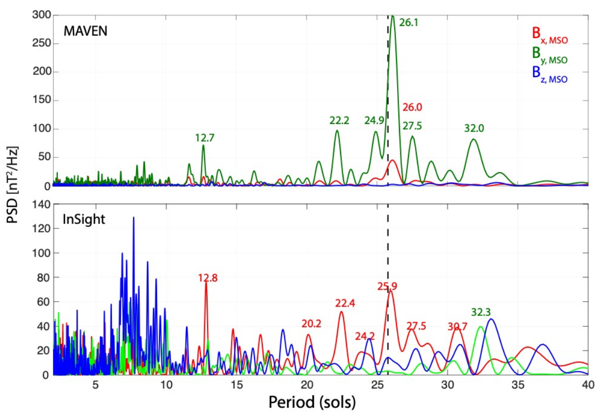

Figure 3 Magnetic field power spectral density in the MSO frame from (upper) MAVEN in the undisturbed IMF data during the time frame of InSight operations, and (lower) IFG.

Daily / harmonics: Focusing on the diurnal signal, we observe the largest amplitude and variability in the East horizontal component (not shown) and with a peak in the early-morning to midmorning. This peak has been shown to occur concurrently with peaks in atmospheric electron density and wind velocity, strengthening the hypothesis that the diurnal variations are dominantly driven by the ionosphere [13].

Short periods: So called ultra-low-frequency (ULF) waves have occurred since the beginning of the mission [2], [11]. These wave phenomena have periods between seconds to minutes and are likely the result of the solar wind interacting with the martian magnetosphere. Continuous pulsations with periodicities around 100 seconds can be observed around midnight while waves around 1000 seconds are mainly observed in the dusk and dawn region.

Transient – Space Weather: The results of a coronal interaction region followed by a coronal mass ejection were observed in December 2020. The event was small and most likely did not fully hit Mars. However, the effect was visible in the magnetic field and overall increased amplitudes and fluctuations were observed following the event [11].

Transient – Dust Movement: Dust movement can lead to triboelectric charging and a magnetic response has been observed on Earth [15]. On Mars, magnetic field signals during individual events of dust movement first identified from imagery were described by [13]. We further performed a systematic investigation of IFG data during the time of pressure drops, indicative of dust lifting events. While magnetic field signatures correlated in time with convective vortices are small and mostly within the noise level, it is likely that triboelectric effects as a result of dust-lifting events are indeed responsible for magnetic field observations [14].

Outlook: Time-varying magnetic fields not only provide information on the interaction of the solar wind/IMF with the planetary/atmospheric obstacle, but can be used to infer interior electrical conductivity structure. Time-varying fields induce currents in the subsurface which in turn lead to an induced response. As such, the observation of external magnetic fields from the surface, paves the way towards magnetic sounding. Further, InSight's magnetometer has enabled observations of time-varying magnetic fields at a specific location, the landing site, over a limited time frame. Including magnetometers on future missions at a variety of locations for long duration continuous observations will be of great value in understanding a range of phenomena and will enable further investigations, including the influence crustal magnetic fields have on ionospheric currents and resulting surface measurements or the effect of space weather during a more active time within the solar cycle.

Acknowledgments: All InSight data used here are publicly available on the Planetary Data System (PDS).

References:

[1] Banerdt, W.B. et al. (2020) *Nature Geo.*, 13, 183. [2] Johnson, C.L. et al. (2020) *Nature Geo.*, 13, 199. [3] Banfield D. et al. (2018) *Space Sci. Rev.*, 214. [4] Smrekar S. et al. (2018) *Space Sci. Rev.*, 215. [5] Mittelholz et al., (2017) *JGR Planets,* 125. [6] Ramstad, R. et al. (2020) *Nature Astronomy*. [7] Brain, D. et al. (2003) *JGR Planets*, 108, 1424. [8] Joy S. P. et al. (2019) *PDS Archive*. [9] Mittelholz, A. et al. (2020) *JGR Planets*, 125. [10] Mittelholz, A. et al. (2021) *LPSC*. [11] Chi, P. et al. (2019) *LPSC*. [12] Mittelholz, A. et al. (2021) *GRL,* 28, 22. [13] Charambalous, C. et al. (2021) *JGR.*, 126. [14] Thorne, S. et al. (2020) *AGU Fall Meeting*. [15] Farrell, W.M. et al. (2004) *JGR*, 109.